Published in final edited form as:
Chem Res Toxicol. 2011 November 21; 24(11): 1924–1936. doi:10.1021/tx200273z.

Polyamines are traps for reactive intermediates in furan metabolism

Lisa A. Peterson[*,†,‡,§], **Martin B. Phillips**[‡,§], **Ding Lu**[‡,‖], and **Mathilde M. Sullivan**[‡]

[†]Division of Environmental Health Sciences, University of Minnesota, Mayo Mail Code 806, 420 Delaware Street SE, Minneapolis, Minnesota 55455

[§]Department of Medicinal Chemistry, University of Minnesota, Mayo Mail Code 806, 420 Delaware Street SE, Minneapolis, Minnesota 55455

[‡]Masonic Cancer Center, University of Minnesota, Mayo Mail Code 806, 420 Delaware Street SE, Minneapolis, Minnesota 55455

Abstract

Furan is toxic and carcinogenic in rodents. Because of the large potential for human exposure, furan is classified as a possible human carcinogen. The detailed mechanism by which furan causes toxicity and cancer is not yet known. Since furan toxicity requires cytochrome P450-catalyzed oxidation of furan, we have characterized the urinary and hepatocyte metabolites of furan to gain insight into the chemical nature of the reactive intermediate. Previous studies in hepatocytes indicated that furan is oxidized to the reactive α,β-unsaturated dialdehyde, *cis*-2-butene-1,4-dial (BDA), which reacts with glutathione (GSH) to form 2-(*S*-glutathionyl)-succinaldehyde (GSH-BDA). This intermediate forms pyrrole cross-links with cellular amines such as lysine and glutamine. In this report, we demonstrate that GSH-BDA also forms cross-links with ornithine, putrescine and spermidine when furan is incubated with rat hepatocytes. The relative levels of these metabolites are not completely explained by hepatocellular levels of the amines or by their reactivity with GSH-BDA. Mercapturic acid derivatives of the spermidine cross-links were detected in the urine of furan-treated rats, which indicates that this metabolic pathway occurs in vivo. Their detection in furan-treated hepatocytes and in urine from furan-treated rats indicates that polyamines may play an important role in the toxicity of furan

Keywords

furan; polyamines; ornithine; metabolism; stable isotope methods; capillary LC-MS; urinary metabolites; GSH; hepatocyte metabolites

INTRODUCTION

Chronic exposure of F344 rats and B6C3F$_1$ mice to furan results in dose-dependent toxicity and carcinogenicity in both species.[1] Furan-treated rats also develop cholangiocarcinomas.[1] Because it is widely distributed in the environment,[2,3] human exposure to furan is likely to be significant. Since there is a large potential for human exposure, furan has been listed by the National Toxicology Program and the International Agency for Research on Cancer as a

[*]To whom correspondence should be addressed. Tel: 612-626-0164. Fax: 612-626-5135. peter431@umn.edu.
[‖]Current address: Department of Pharmacology, University of Pennsylvania, Philadelphia, PA 19104.

Supporting Information Available. Supplementary table and figures. This material is available free of charge via the Internet at http://pubs.acs.org.

possible human carcinogen (Group 2B).[2,4] Adequate human risk assessment has been stymied because of the lack of mechanism-based biomarkers.

Furan requires metabolism by cytochrome P450 2E1 to elicit its toxic effects.[5,6] Chemical characterization of the metabolites of furan provides insights into the identity of the reactive intermediates formed as a result of furan metabolism. The initial product of furan oxidation is *cis*-2-butene-1,4-dial (BDA, Scheme 1).[7,8] The metabolites characterized to date in urine from furan-exposed rats indicate that BDA reacts with cellular nucleophiles such as glutathione (GSH), cysteine and lysine (Scheme 1).[9-12] The majority of the urinary metabolites are derived from a cysteine-BDA-lysine cross-link, *S*-[1-(5-amino-5-carboxypentyl)-1*H*-pyrrol-3-yl]-L-cysteine (**1**, Cys-BDA-lysine, Scheme 1).[10-12] Studies in rat hepatocytes indicate that a major source of metabolite **1** is a GSH-BDA-lysine cross-link, *S*-[1-(5-amino-5-carboxypentyl)-1*H*-pyrrol-3-yl]-glutathione (**2**, GSH-BDA-lysine, Scheme 1).[11] This observation suggests that once BDA is formed, it reacts with GSH to form 2-(*S*-glutathionyl)succinaldehyde (GSH-BDA, **3**), which reacts with lysine to form the observed GSH-BDA-lysine cross-link (Scheme 1). This cross-link is then further processed to the urinary metabolites.

Lysine is not the only target for this cross-linking reaction. Intramolecular cross-linking occurs to form *N*-[4-carboxy-4-(3-mercapto-1*H*-pyrrol-1-yl)-1-oxobutyl]-L-cysteinylglycine cyclic sulfide (mono-GSH-BDA, **4**, Scheme 1). Cross-links with glutamine and several other unidentified GSH conjugates were also observed in media from rat hepatocytes exposed to furan.[11] In this report, we provide the chemical identity for five of these unidentified metabolites. They result from the reaction of GSH-BDA **3** with the primary amino groups of ornithine, spermidine and putrescine. These findings led to the characterization of related metabolites in the urine of furan-treated rats. Polyamines are critical for normal cell growth and function.[13] The cellular levels of these compounds are maintained through a tightly regulated network of enzymes involved in their formation and degradation. Imbalance in polyamine pathways is associated with a number of diseases, including cancer.[14-16] The formation of GSH-BDA-polyamine reaction products indicates that polyamines are traps for electrophilic furan metabolites and suggests pathways, in addition to DNA and protein adduct formation, for furan to exert its toxic effects.

EXPERIMENTAL PROCEDURES

Caution: *BDA is toxic and mutagenic in cell systems. Furan is toxic and carcinogenic in laboratory animals. Both chemicals should be handled with proper safety equipment and precautions*.

Chemicals

[$^{13}C_4$]Furan, BDA, mono-GSH-BDA (**4**) and GSH-BDA-GSH conjugates were prepared as previously described.[9,17-19] The concentration of aqueous solutions of BDA was determined as previously described.[20] Furan was purchased from Acros Organics (Pittsburgh, PA) and distilled before use. Spermine, cadaverine, and putrescine were purchased from MP Biomedicals (Solon, OH). All other reagents were purchased from Aldrich Chemical (Milwaukee, WI) unless stated otherwise. All HPLC solvents were chromatography grade.

Instrumentation

HPLC purifications were carried out on a Shimadzu LC-10AD system coupled to a Shimadzu SCL-10A UV/vis detector. NMR spectra were recorded on 500 or 600 MHz Varian Inova spectrometers or a 700 MHz Bruker Avance spectrometer in the Department of Chemistry or the Department of Biochemistry, Molecular Biology, and Biophysics,

University of Minnesota. Chemical shifts are reported in parts per million (ppm) as referenced to the residual solvent peak.

Collision-induced mass spectra of reaction products were obtained on an Agilent 1100 series LC/MSD Trap SL mass spectrometer operating in positive ion mode. Each compound was dissolved in 10 mM ammonium formate, pH 2.8, and directly infused into the ion source. Helium was the nebulizing and drying gas (15 psi, 5 L/min) which had a temperature set at 200 °C. High resolution mass spectral data for the synthetic standards were obtained on a Bruker BioTOF II mass spectrometer in the Department of Chemistry, University of Minnesota or a Thermo Ultra AM Triple Quadrupole mass spectrometer in the Masonic Cancer Center, University of Minnesota.

For most of the HPLC and LC-MS analyses, the column was eluted with the following gradient: 10 min at 100% A; 26 min gradient to 75% A, 25% B; 10 min gradient to 50% A, 50% B; 4 min gradient to 100% B where solvent A was 10 or 50 mM ammonium formate, pH 2.8 and solvent B was 50% acetonitrile in water. This gradient will subsequently be referenced as HPLC method 1.

Reactions between GSH, BDA, and Amines

GSH (21 mg, 68 μmol) and L-ornithine hydrochloride (11 mg, 68 μmol), putrescine (6.0 mg, 68 μmol), spermidine (9.8 mg, 68 μmol), spermine (14 mg, 68 μmol) or cadaverine (6.9 mg, 68 μmol) were added to a solution of BDA (68 μmol) in 50 mM or 1 M sodium phosphate, pH 7.4 (total volume: 2 mL). After 2 h at 37 °C, the products were purified on a semipreparative Phenomenex (Torrence, CA) Synergi 4μ Hydro-RP column (250 × 10 mm, 4 μm) employing HPLC method 1 (solvent A was 50 mM ammonium formate, pH 2.8) with a flow rate of 4 mL/min. The eluting peaks were collected and concentrated under reduced pressure. The buffer salts were removed by HPLC purification as described for each compound.

GSH-BDA-Ornithine—When the reaction was performed with ornithine, the resulting reaction mixture was complex. However, there were two prominent UV-absorbing products in a ratio of 5:7 whose mass spectra had a molecular ion at *m/z* 488. This mass is consistent with the formation of a cross-link between ornithine and GSH via BDA. Mass spectral analysis indicated that the other peaks were either GSH-BDA reaction products (*m/z* 356, GSH-BDA $[M+H^+]$) or further BDA or GSH-BDA reaction products of GSH-BDA-ornithine (*m/z* 554, GSH-2BDA-ornithine $[M+H^+]$ or *m/z* 422, 2GSH-2BDA-ornithine $[M+2H]^{2+}$). The two GSH-BDA-ornithine products eluted at 22.8 min and 27.7 min when HPLC method 1 was employed (solvent A was 50 mM ammonium formate, pH 2.8). Following preparative isolation by HPLC, they were desalted on a semipreparative Synergi 4μ Hydro-RP column with the following gradient (4 mL/min): 5 min at 100% A; 20 min gradient to 85% A, 15% B; 5 min gradient to 70% A, 30% B where solvent A was 0.1% v/v formic acid and solvent B was 50 % acetonitrile in water. The compound that eluted at 22.8 min was identified as *S*-[1-(4-amino-1-carboxybutyl)-1*H*-pyrrol-3-yl]-glutathione (GSH-BDA-N^{α}-ornithine). ^{1}H NMR (500 MHz, D_2O): δ 6.88 (s, 1H, H2’), 6.71 (s, 1H, H5’), 6.19 (s, 1H, H4’), 4.45 (dd, 1H, H1), 4.25 (dd, 1H, Cys α-CH), 3.70 (m, 1H, Glu α-CH), 3.64 (s, 2H, Gly α-CH_2), 3.12 (dd, 1H, Cys β-CH_a), 2.92 (m, 2H, H4), 2.80 (dd, 1H, Cys β-CH_b), 2.47 (m, 2H, Glu γ-CH_2), 2.13–2.08 (m, 3H, Glu β-CH_2, $H2_a$), 1.96 (m, 1H, $H2_b$), 1.57 (m, 1H, $H3_a$), 1.41 (m, 1H, $H3_b$). MS data are displayed in Table 1.

The compound that eluted at 27.7 min was characterized as *S*-[1-(4-amino-4-carboxybutyl)-1*H*-pyrrol-3-yl]-glutathione (GSH-BDA-N^{δ}-ornithine). ^{1}H NMR (500 MHz, D_2O): δ 6.77 (s, 1H, H5’), 6.16 (d, 1H, H4’), 4.29 (m, 1H Cys α-CH), 3.90 (m, H4), 3.80 (s, 2H, Gly α-CH_2), 3.74 (m, 1H, Glu α-CH), 3.69 (m, 1H, H1), 3.09 (dd, 1H, Cys β-CH_a), 2.83

(dd, 1H, Cys β-CH_b), 2.45 (m, 2H, Glu γ-CH_2), 2.09 (m, 2H, Glu β-CH_2), 1.80 (m, 1H, $H3_a$), 1.72–1.70 (m, 3H, $H3_b$ and H2). MS data are displayed in Table 1.

GSH-BDA-Spermidine—The GSH-BDA-spermidine reaction mixture contained multiple products. Two UV-absorbing products had the expected molecular ions at *m/z* 501. These products, which eluted at 24.5 and 28.1 min, were present in a ratio of 4:1 (HPLC Method 1, solvent A was 50 mM ammonium formate, pH 2.8). Based on mass spectral analysis, the other peaks were either GSH-BDA reaction products (m/z 356, GSH-BDA [$M+H^+$]) or further reaction products of GSH-BDA-spermidine with additional molecules of BDA (*m/z* 567, GSH-2BDA-spermidine [$M+H^+$] or *m/z* 633, GSH-3BDA-spermine [$M+H^+$]). The GSH-BDA-spermidine reaction products were purified by semipreparative HPLC (HPLC method 1, 50 mM ammonium formate, pH 2.8) and the collected products were desalted for NMR analysis on a semipreparative Synergi 4μ Hydro-RP column with the following gradient (4 mL/min). 5 min at 100% A; 15 min gradient to 85% A, 15% B; 5 min gradient to 70% A, 30% B where solvent A was 0.1% v/v formic acid and solvent B was 50 % acetonitrile in water. The major isomer that eluted at 24.5 min was identified as *N*-(3-(3-(*S*-glutathionyl)-1*H*-pyrrol-1-yl)propyl)butane-1,4-diamine (GSH-BDA-N^1-spermidine). ^{1}H NMR (500 MHz, D_2O): 6.68 (s, 1H, H5'), 6.10 (s, 1H, H4'), 4.17 (dd, 1H, Cys α-CH), 3.88 (t, 2H, H1), 3.63 (t, 1H, Glu α-CH), 3.54 (s, 2H, Gly α-CH_2), 3.01 (dd, 1H, Cys β-CH_a), 2.93–2.83 (m, 4H, H4 and H7), 2.81–2.70 (m, 3H, H3, Cys β-CH_b), 2.38 (m, 2H, Glu γ-CH_2), 2.02–1.93 (m, 4H, Glu β-CH_2, H2), 1.56 (m, 4H, H5 and H6). MS data are displayed in Table 1.

The minor isomer that eluted at 28.1 min was identified as *N*-(4-(3-(*S*-glutathionyl)-1*H*-pyrrol-1-yl)butyl)propane-1,3-diamine (GSH-BDA-N^8-spermidine). ^{1}H NMR (500MHz, D_2O): δ 6.67 (s, 1H, H5'), 6.08 (s, 1H, H4'), 4.14 (dd, 1H, Cys α-CH), 3.80 (t, 2H, H1), 3.63 (t, 1H, Glu α-CH), 3.58 (s, 2H, Gly α-CH_2), 3.00 (dd, 1H, Cys β-CH_a), 2.96–2.88 (m, 4H, H5 and H7), 2.83 (t, 2H, H4), 2.71 (dd, 1H, Cys β-CH_b), 2.38 (m, 2H, Glu γ-CH_2), 2.01 (q, 2H, Glu β-CH_2), 1.88 (m, 2H, H6), 1.66 (m, 2H, H2), 1.42 (m, 2H, H3). MS data are displayed in Table 1.

GSH-BDA-Cadaverine—A single UV-absorbing compound with a molecular ion of *m/z* 458 was observed in the GSH-BDA-cadaverine reaction mixture. This compound eluted at 35.2 min when HPLC method 1 was employed (solvent A was 50 mM ammonium formate, pH 2.8). The HPLC purified product was desalted on a semipreparative Synergi 4μ Hydro-RP column with the following gradient (4 mL/min): 5 min at 100% A; 10 min gradient to 75% A, 25% B; 5 min gradient to 25% A, 75% B where solvent A was 0.1% v/v formic acid/water and solvent B was 50% acetonitrile in water. The product was identified as *S*-(1-(5-aminopentyl)-1*H*-pyrrol-3-yl)glutathione (GSH-BDA-cadaverine). ^{1}H NMR (500 MHz, DMSO-d_6): δ 6.84 (s, 1H, H2'), 6.77 (s, 1H, H5'), 6.07 (s, 1H, H4'), 4.24 (dd, 1H, Cys α-CH), 3.84 (m, 2H, H1), 3.55 (m, 2H, Gly α-CH_2), 3.45 (m, 1H, Glu α–CH), 2.95 (dd, 1H, Cys β-CH_a), 2.75 (t, 2H, H5), 2.63 (dd, 1H, Cys β-CH_b), 2.35 (m, 2H, Glu γ-CH_2), 1.97 (m, 2H, Glu β-CH_2), 1.63 (m, 2H, H2), 1.54 (m, 2H, H4), 1.20 (m, 2H, H3). MS data are displayed in Table 1.

GSH-BDA-Putrescine—In the reaction mixture of GSH-BDA-putrescine, one UV absorbing compound was observed with the expected molecular ion of *m/z* 444. This compound eluted at 30.5 min when HPLC method 1 was employed (solvent A was 50 mM ammonium formate, pH 2.8). Fractions containing this compound were desalted on a semipreparative Synergi 4μ Hydro-RP column with the following gradient (4 mL/min): 5 min at 100% A; 10 min gradient to 75% A, 25% B; 5 min gradient to 25% A, 75% B where solvent A was 0.1% v/v formic acid/water and solvent B was 50% acetonitrile in water. It was identified as *S*-(1-(4-aminobutyl)-1*H*-pyrrol-3-yl)glutathione (GSH-BDA-

putrescine). ^{1}H NMR (500 MHz, D_2O): δ 6.76 (m, 1H, H2'), 6.68 (m, 1H, H5'), 6.07 (m, 1H, H4'), 4.18 (dd, 1H, Cys α-CH), 3.80 (t, 2H, H1), 3.62 (t, 1H, Glu α-CH), 3.57 (m, 2H, Gly α-CH_2), 3.01 (dd, 1H, Cys β-CH_a), 2.77 (m, 2H, H4), 2.73 (dd, 1H, Cys β-CH_b), 2.37 (m, 2H, Glu γ-CH_2), 2.01 (m, 2H, Glu β-CH_2), 1.66 (m, 2H, H2), 1.42 (m, 2H, H3). MS data are displayed in Table 1.

GSH-BDA-Spermine—One UV-absorbing compound with the expected molecular ion of *m/z* 558 was observed in the reaction mixture containing GSH, BDA, and spermine. This compound eluted at 27.8 min when HPLC method 1 was employed (solvent A was 50 mM ammonium formate, pH 2.8). Fractions containing this reaction product were desalted with HPLC method 1. It was identified as *N*-(3-((*S*-glutathionyl)-1*H*-pyrrol-1-yl)propyl)butane-1,4-diamine (GSH-BDA-spermine). ^{1}H NMR (500 MHz, D_2O): δ 6.75 (s, 1H, H2'), 6.67 (m, 1H, H5'), 6.09 (m, 1H, H4'), 4.14 (dd, 1H, Cys α-CH), 3.87 (t, 2H, H1), 3.63 (t, 1H, Glu α–CH), 3.57 (d, 2H, Gly α–CH_2), 3.01 (m, 1H, Cys β–CH_a), 2.98–2.82 (m, 8H, H4, H7, H8, H10), 2.77–2.68 (m, 3H, Cys β-CH_b, H3), 2.38 (m, 2H, Glu γ-CH_2), 2.05–1.86 (m, 6H, Glu β-CH_2, H2, H9), 1.61–1.49 (m, 4H, H5, H6). MS data are displayed in Table 1.

Reaction between NAC, BDA, and L-ornithine

N-Acetyl-L-cysteine (NAC) (8 mg, 50 μmol) and BDA (50 μmol) were incubated in 1 mL of 1 M sodium phosphate, pH 7.4, at 37 °C for 30 min before adding L-ornithine monohydrochloride (8 mg, 50 μmol). The reaction was stirred for 15 hours. LC-MS analysis of the reaction mixture with HPLC method 1 demonstrated two major peaks (*m/z* 344) eluting at 37.0 min and 50.3 min. MS data are displayed in Table 1.

Reaction between NAC, BDA, and spermidine

NAC (45 mg, 270 μmol) and BDA (135 μmol) were incubated in 3 mL of 1 M sodium phosphate, pH 7.4, at 37 °C for 25 min before adding spermidine (39 mg, 270 μmol). The reaction was stirred for 15 hours. HPLC analysis of the reaction mixture with HPLC method 1 demonstrated two major UV-absorbing peaks eluting at 32.0 min and 37.1 min in a ratio of 6:1. The two diastereomers (*m/z* 357) were purified by semipreparative HPLC. The organic solvent was removed under reduced pressure and the buffer salt was removed by solid phase extraction using Strata-X cartridges.

The first compound that eluted at 32.0 min was identified as *N*-acetyl-*S*-[1-(3-((4-aminobutyl)amino)propyl)-1*H*-pyrrol-3-yl]-L-cysteine (NAC-BDA-N^1-spermidine). ^{1}H NMR (500 MHz, D_2O): δ 6.75 (s, 1H, H2'), 6.67 (t, 1H, *J*=2.5 Hz, H5'), 6.09 (t, 1H, *J*=2.5 Hz, H4'), 4.03 (dd, 1H, *J*=4.0, 9.5, Cys α-CH), 3.86 (dd, 2H, *J*=5.0, 6.5 Hz, H1), 3.03-3.00 (m, 1H, Cys β-CH_a), 2.89-2.82 (m, 4H, H4 and H7), 2.77 (t, 2H, *J*=7.5 Hz, H3), 2.72-2.67 (m, 1H, Cys β-CH_b), 2.00-1.96 (m, 2H, H2), 1.86 (s, 3H, Ac), 1.58-1.52 (m, 4H, H5 and H6). MS data are displayed in Table 1.

The compound that eluted at 37.1 min was identified as *N*-acetyl-*S*-[1-(4-((3-aminobutyl)amino)propyl)-1*H*-pyrrol-3-yl]-L-cysteine (NAC-BDA-N^8-spermidine). ^{1}H NMR (700 MHz, D_2O): δ 6.83 (s, 1H, H2'), 6.75 (s, 1H, H5'), 6.16 (s, 1H, H4'), 4.12-4.08 (m, 1H, Cys α-CH), 3.88-3.84 (m, 2H, H1), 3.11-3.08 (m, 1H, Cys β-CH_a), 2.99-2.93 (m, 4H, H5 and H7), 2.88-2.85 (m, 2H, H4), 2.78-2.74 (m, 1H, Cys β-CH_b), 1.98-1.93 (m, 2H, H6), 1.96 (s, 3H, Ac), 1.75-1.65 (m, 2H, H2), 1.52-1.46 (m, 2H, H3). MS data are displayed in Table 1.

General procedure for the synthesis of sulfoxide standards

m-Chloroperbenzoic acid (mCPBA) (3 μmol) was added to a stirred solution of the corresponding sulfide (3 μmol) in methanol-dichloromethane (1:1) at -78 °C (total volume: 1 mL). The reaction was stirred for 1 h before it was allowed to warm up to room temperature. The solvent was removed under a stream of nitrogen. The crude product was dissolved in water and purified by semipreparative HPLC method 1 (solvent A was 50 mM ammonium formate, pH 2.8). The organic solvent was removed under reduced pressure, and buffer salts were removed by solid phase extraction using Strata-X cartridges. The identities of products were established by MS and NMR analysis.

N-*Acetyl*-S-*[1-(3-(4-aminobutyl)aminopropyl)-1*H-*pyrrol-3-yl]*-L-*cysteine sulfoxide—NAC-BDA-N^1-spermidine was oxidized with mCPBA to generate *N*-acetyl-*S*-[1-(3-(4-aminobutyl)aminopropyl)-1*H*-pyrrol-3-yl]-L-cysteine sulfoxide. This product eluted at 3.7 min when HPLC method 1 was employed (solvent A was 50 mM ammonium formate). ^{1}H NMR analysis showed the presence of two diastereomers in a 6:5 ratio. MS data are displayed in Table 1.

Major isomer: ^{1}H NMR (700 MHz, DMSO-d_6): δ 7.88 (d, 1H, *J*=8.2 Hz, NH), 7.30 (s, 1H, H2'), 6.95 (s, 1H, H5'), 6.39 (s, 1H, H4'), 4.04-4.01 (m, 2H, H1), 3.79-3.76 (m, 1H, Cys α-CH), 3.30 (dd, 1H, *J*=3.1, 12.2 Hz, Cys β-CH_a), 3.07 (t, 1H, *J*=10.6 Hz, Cys β-CH_b), 2.74-2.72 (m, 2H, H4), 2.57-2.55 (m, 2H, H7), 2.41-2.38 (m, 2H, H3), 1.91-1.88 (m, 2H, H), 1.79 (s, 3H, - C(O)-CH_3), 1.54-1.52 (m, 2H, H5), 1.46-1.44 (m, 2H, H6).

Minor isomer: ^{1}H NMR (700 MHz, DMSO-d_6): δ 7.74 (d, 1H, J=7.7 Hz, NH), 7.30 (s, 1H, H2'), 6.92 (s, 1H, H5'), 6.36 (s, 1H, H4'), 4.20-4.17 (m, 1H, Cys α-CH), 4.04-4.01 (m, 2H, H1), 3.37-3.35 (m, 1H, Cys β-CH_a), 2.97-2.94 (m, 1H, Cys β-CH_b), 2.74-2.72 (m, 2H, H4), 2.57-2.55 (m, 2H, H7), 2.41-2.38 (m, 2H, H3), 1.91-1.88 (m, 2H, H), 1.83 (s, 3H, -C(O)-CH_3), 1.54-1.52 (m, 2H, H5), 1.46-1.44 (m, 2H, H6).

N-*Acetyl*-S-*[1-(4-(3-aminobutyl)aminopropyl)-1*H-*pyrrol-3-yl]*-L-*cysteine sulfoxide—NAC-BDA-N^8-spermidine was oxidized with mCPBA to generate *N*-acetyl-*S*-[1-(4-(3-aminobutyl)aminopropyl)-1*H*-pyrrol-3-yl]-L-cysteine sulfoxide. This product eluted at 3.5 min when HPLC method 1 was employed. ^{1}H NMR analysis showed the presence of two diastereomers in a 6:5 ratio. MS data are displayed in Table 1.

Major isomer: ^{1}H NMR (700 MHz, DMSO-d_6): δ 7.86 (d, 1H, *J*=8.1 Hz, NH), 7.42 (s, 1H, H2'), 6.94 (s, 1H, H5'), 6.35 (s, 1H, H4'), 4.18-4.16 (m, 1H, Cys α-CH), 4.06-3.96 (m, 2H), 3.59-3.57 (m, 1H, Cys β-CH_a), 3.27-3.24 (m, 1H, Cys β-CH_b), 2.86-2.70 (m, 4H), 2.62-2.60 (m, 2H), 1.81 (s, 3H, -C(O)-CH_3), 1.81-1.69 (m, 4H), 1.36-1.30 (m, 1H), 1.27-1.21 (m, 1H).

Minor isomer: ^{1}H NMR (700 MHz, DMSO-d_6): δ 8.05 (d, 1H, *J*=8.2 Hz, NH), 7.29 (s, 1H, H2'), 6.96 (s, 1H, H5'), 6.40 (s, 1H, H4'), 4.06-3.96 (m, 2H), 3.72-3.70 (m, 1H, Cys α-CH), 3.23-3.15 (m, 1H, Cys β-CH_a), 3.08-3.05 (m, 1H, Cys β-CH_b), 2.86-2.70 (m, 4H), 2.62-2.60 (m, 2H), 1.83 (s, 3H, -C(O)-CH_3), 1.81-1.69 (m, 4H), 1.36-1.30 (m, 1H), 1.27-1.21 (m, 1H).

Hepatocyte Incubations

Freshly isolated hepatocytes were prepared from F344 rats according to published methods.[21] The viability of the cells was greater than 85% as judged by trypan blue exclusion. The hepatocyte incubations were performed in sealed screw-capped 25 mL Erlenmeyer flasks to prevent furan evaporation as previously reported.[5] The cells were suspended at a concentration of 2 million cells/mL in RPMI 1640 media, containing 10 mM HEPES, pH 7.4. After a 10 min preincubation period at 37 °C in an atmosphere of 5% CO_2,

the flasks were capped tightly and a solution of furan was added with a syringe through a septum to a final concentration of 100 μM. Controls were performed in the absence of furan or in the presence of 200 μM 1-phenylimidazole (an inhibitor of CYP2E1). The mixtures were then incubated at 37 °C with gentle shaking. After 4 h, the mixture was centrifuged at 6000 × *g* for 5 min. The supernatant was removed and stored at -20 °C for LC/MS/MS analysis. Incubations were performed in duplicate and were repeated with different hepatocyte preparations. The supernatants from the incubations were directly analyzed by LC/MS for metabolites.

Animal Studies

All procedures involving the use of animals in these studies were approved by the University of Minnesota Institutional Animal Care and Use Committee and performed according to NIH guidelines. F344 male rats (200-300 g) were purchased from Charles River Laboratories (Kingston, NY). Groups of three rats were treated with 8 mg/kg [$^{12}C_4$]- or [$^{13}C_4$]furan in 5 mL/kg corn oil by gavage. The control group received only corn oil. Immediately after treatment, rats were transferred to individual metabolism cages according to NIH guidelines. Urine was collected on dry ice for 24 hours and stored at -80 °C. Prior to MS analysis, it was acidified with TFA to a final concentration of 2% (v/v), centrifuged to remove any particulate matter, and filtered through a 0.45 μm syringe filter.

LC/MS Analysis of Metabolites

LC/MS/MS analyses of supernatants from hepatocyte incubations, in vitro reaction mixtures, or urine were conducted with a Phenomenex (Torrence, CA) Synergi Hydro-RP 80Å column (250 mm × 0.5 mm, 4 μm) at a flow rate of 12.5 μL/min. The column was eluted with HPLC method 1 (solvent A was 10 mM ammonium formate, pH 2.8). The HPLC was coupled to an Agilent 1100 series LC/MSD Trap SL mass spectrometer operating in positive ion mode. Helium was the nebulizing and drying gas (15 psi, 5 L/min), and had a temperature set at 200 °C. Initial analyses were performed with the mass spectrometer set to full scanning mode with a scan range of 75-750 *m/z*. The resulting data were mined for compounds that were present in the furan-exposed samples and absent in the control samples. The samples were then reanalyzed with the mass spectrometer set in the auto-MS^2 mode to obtain fragmentation patterns for each of the metabolites.

For a more sensitive scan of the hepatocyte supernatants and synthetic standards, LC/MS/MS analyses were conducted on a nanoACQUITY UPLC pump (Waters, Milford, MA) coupled to a Finnigan TSQ Quantum Ultra AM mass spectrometer (Thermo Electron, San Jose, CA) operating in positive mode. The compounds were separated on a Phenomenex Synergi Hydro-RP 80Å column (250 mm × 0.5 mm, 4 μm) at a flow rate of 10 μL/min. The column was eluted with the following gradient: 10 min at 100% A; 15 min gradient to 75% A, 25% B; 5 min gradient to 50% A, 50% B; 5 min gradient to 100% B, where solvent A was 10 mM ammonium formate, pH 2.8, and solvent B was 50% acetonitrile in water. Selected reaction monitoring (neutral loss 129) was used to target for specific GSH-BDA-amine cross-links.

To detect metabolites with unknown parent masses but known structure (NAC and NAC sulfoxide conjugates), LC/MS/MS analyses were conducted on a nanoACQUITY UPLC pump (Waters, Milford, MA) coupled to a Finnigan TSQ Quantum Ultra AM mass spectrometer (Thermo Electron, San Jose, CA) operating in positive ion mode. The compounds were separated at a flow rate of 10 μL/min on a Phenomenex Synergi Hydro-RP 80Å column (250 mm × 0.5 mm, 4 μm) with HPLC method 1 (solvent A was 10 mM ammonium formate, pH 2.8). The mass spectrometer was operated in constant neutral loss (CNL) mode with a scan range (parent mass) of 300-450 *m/z*. A neutral loss of 129 was used

for NAC conjugates, while a neutral loss of 177 was used for the NAC sulfoxide conjugates.[10,11]

High resolution mass spectral data for the metabolites were obtained on a Thermo Ultra AM Triple Quadrupole mass spectrometer. The compounds were separated on a Phenomenex Synergi Hydro-RP 80Å column (250 mm × 0.5 mm, 4 μm) using a flow rate of 10 μL/min. The column was eluted with HPLC method 1 where solvent A was 0.1% (v/v) phosphoric acid in water and solvent B was 1% (v/v) phosphoric acid in water containing 50% acetonitrile. Selected reaction monitoring (SRM) experiments were performed using the same instrumentation, but the column was eluted with HPLC Method 1 (solvent A was 10 mM ammonium formate, pH 2.8) with a flow rate of 15 μL/min. Argon was used as the collision gas with a collision energy set at 15 eV.

In vitro relative reactivity experiments

GSH (1.5 mg, 5 μmol) and an equimolar mixture of putrescine, cadaverine, L-ornithine, spermine, spermidine, and L-lysine (100 nmol each) were combined in a 1.5 mL amber vial with either sodium phosphate buffer (150 mM, pH 7.4) or hepatocyte medium (total volume: 1 mL). The reaction was initiated upon addition of BDA (100 nmol). After 90 min at 37 °C, the reaction mixture was analyzed by LC/MS (flow rate 12 μL/min) using HPLC method 1 (solvent A was 10 mM ammonium formate, pH 2.8) to determine the relative levels of the GSH-BDA-amine reaction products.

The data were corrected for differences in ionization. This was determined as follows: Equimolar amounts of GSH, BDA, and an amine (putrescine, cadaverine, L-ornithine, spermine, spermidine, or L-lysine) were combined in 150 mM sodium phosphate buffer, pH 7.4. The GSH-BDA-amine reaction products were isolated by HPLC and desalted as described above. The identity of products was established by MS analysis. Assuming that the molar extinction coefficient of each product was similar, the GSH-BDA-amine fractions were combined into an equimolar mixture of each product. This generated an HPLC trace that contained equal peak areas for all the GSH-BDA-amine products using analytical HPLC Method 1. The mixture was diluted 1:10 into three different solutions: water, hepatocyte media, or 150 mM sodium phosphate buffer (pH 7.4). These diluted solutions were analyzed by LC/MS using HPLC Method 1 (flow rate 12 μL/min). The ratio of the area of each peak to the sum of all peaks was calculated. This ratio was divided by 1/9 (≈11.1%), which is the expected ratio if each of the nine isomers gave an identical response. The resulting fraction is the correction factor listed in Supplemental Table 1.

RESULTS

Hepatocyte metabolites

Previously, we reported that freshly isolated hepatocytes convert furan to several metabolites, including GSH-BDA cross-links to the α- and ε-amino groups of lysine and a GSH-BDA cross-link to glutamine (*S*-[1-(4-amino-1-carboxy-4-oxobuty)-1*H*-pyrrol-3-yl]-glutathione, GSH-BDA-glutamine, **5**, Scheme 2).[11] Constant neutral loss (CNL) analysis of the LC-MS/MS data of hepatocyte supernatants indicated the presence of several additional glutathione reaction products (Figure 1). The formation of these metabolites required furan and was blocked upon inclusion of 1-phenylimidazole, a selective cytochrome P450 2E1 inhibitor.[22] Our hypothesis was that these metabolites were GSH-BDA cross-links with cellular amines similar to GSH-BDA-lysine or GSH-BDA-glutamine.

The metabolite with the largest area had a molecular ion at *m/z* 488 (Figure 1). Extraction of the ion current at 488 m/z indicated the presence of two metabolites (Supplemental Figure 1a). This nominal mass of these metabolites is 14 amu less than the GSH-BDA-lysine and

GSH-BDA-glutamine cross-links. Two amino acids with the appropriate molecular weight are asparagine and ornithine. Reaction of asparagine with BDA in the presence of GSH generated the formation of one major and one minor reaction product with molecular ions of *m/z* 488. The major isomer was likely the cross-link with the α-amino group as was observed with glutamine (**6**, Scheme 2).[11] Preliminary studies indicated that the hepatocyte metabolites did not co-elute with these reaction products (data not shown) so we did not chemically characterize these products.

Ornithine also reacts with BDA in the presence of GSH to form two reaction products with molecular ions at *m/z* 488. These compounds co-eluted with the hepatocyte metabolites (Supplemental Figure 1a). Preparative scale isolation and chemical characterization of the GSH-BDA-ornithine reaction products indicated that the first eluting product results from pyrrole formation with the α-amino group (*S*-[1-(4-amino-1-carboxybutyl)-1*H*-pyrrol-3-yl]-glutathione, GSH-BDA-N^{α}-ornithine, **7a**, Scheme 2) and the second eluting product has the cross-link occurring on the δ-amino group (*S*-[1-(4-amino-4-carboxybutyl)-1*H*-pyrrol-3-yl]-glutathione, GSH-BDA-N^{δ}-ornithine, **7b**) (Supplemental Figure 2). These standards had the same exact mass and MS^2 fragmentation pattern as the metabolites (Table 1, Supplemental Figure 1b).

Another metabolites detected in the CNL 129 mass chromatogram had molecular ion at *m/z* 501 (Figure 1). Extraction of *m/z* 501 indicated the presence of two metabolites with this mass (Supplemental Figure 3a). This mass is consistent with the formation of GSH-BDA cross-links with spermidine which has a nominal mass of 145 Da. Reaction of BDA with spermidine and GSH generated two GSH-BDA-spermidine products with molecular ions of *m/z* 501 that co-eluted with the hepatocyte metabolites (Supplemental Figure 3a). COSY NMR analysis of the chemical reaction products indicated that the first eluting product resulted from the cross-link being formed with the primary amine attached to the three-carbon chain (*N*-(3-(3-(*S*-glutathionyl)-1*H*-pyrrol-1-yl)propyl)butane-1,4-diamine, GSH-BDA-N^1-spermidine, **8a**, Scheme 2) and the later eluting product resulted from cross-link formation with the primary amino group attached to the four-carbon chain (*N*-(4-(3-(*S*-glutathionyl)-1*H*-pyrrol-1-yl)butyl)propane-1,3-diamine, GSH-BDA-N^8-spermidine, **8b**, Scheme 2) (Supplemental Figure 4). The MS^2 fragmentation and exact mass of the metabolites matched those of the synthetic standards (Table 1, Supplemental Figure 3b).

After observing that GSH-BDA (**3**) reacts with spermidine to form cross-links, we prepared the synthetic standards for the GSH-BDA cross-links to the other polyamines, putrescine, spermine and cadavarine. Reaction of GSH-BDA (**3**) with putrescine generates a single cross-link with a molecular ion of *m/z* 444 (Table 1, Supplemental Figure 5). NMR analysis confirmed the structure as *S*-(1-(4-aminobutyl)-1*H*-pyrrol-3-yl)glutathione (GSH-BDA-putrescine, **9**, Scheme 2). This metabolite was not observed when the hepatocyte medium was analyzed by LC/MS/MS on the ion trap mass spectrometer. However, when the hepatocyte medium was analyzed by selected reaction monitoring (SRM) for the transition of *m/z* 444 → *m/z* 315 (neutral loss of 129) on a triple quadrupole mass spectrometer, a peak with a similar retention time to the synthetic standard was observed (Figure 2). Subsequently, we demonstrated that this metabolite co-eluted with the synthetic standard (Figure 2).

GSH-BDA (**3**) reacts with spermine or cadaverine to form single reaction products with molecular ions at *m/z* 558 and 458, respectively (Table 1). NMR analysis confirmed the structures as *N*-(3-((*S*-glutathionyl)-1*H*-pyrrol-1-yl)propyl)butane-1,4-diamine (GSH-BDA-spermine, **10**) and *S*-(1-(5-aminopentyl)-1*H*-pyrrol-3-yl)glutathione (GSH-BDA-cadaverine, **11**, Scheme 2). Neither compound was observed in the hepatocyte medium even when SRM

analysis on a triple quad mass spectrometer was performed (**10**: *m/z* 558 → *m/z* 429 or **11**: *m/z* 458 → *m/z* 329; data not shown).

Urinary Metabolites

Since GSH-BDA (**3**) cross-links with ornithine, spermidine and putrescine were observed as rat hepatocyte metabolites of furan, we investigated whether the *N*-acetyl-L-cysteine (NAC) derivatives of these compounds were present in the urine from furan-treated rats. The mercapturates were targeted since the major metabolites detected in the urine thus far had been NAC-BDA-lysine metabolites.[11,12] We focused on the ornithine and spermidine cross-links since they were the most abundant hepatocyte metabolites. Standards for the NAC-BDA-amine cross-links were prepared by combining the amine with BDA in the presence of NAC.

Two ornithine reaction products (*m/z* 344) were formed when NAC, BDA and ornithine were combined, eluting at 37 and 50 minutes (Table 1). In the urine of furan-treated rats, there were no peaks unique to furan exposure with this mass, even when analyzed by SRM (*m/z* 344 → *m/z* 197 and *m/z* 344 → *m/z* 215; data not shown).

When BDA was combined with spermidine and NAC, two major UV-absorbing peaks were observed in the HPLC trace, eluting at 32.0 min and 37.1 min in a ratio of 6:1. Mass spectral analysis demonstrated that they had the expected molecular ion (*m/z* 357) for the NAC-BDA-spermidine cross-links (Table 1). Preparative isolation and characterization by NMR analysis indicated that the peak that elutes at 32.0 min is the spermidine-N^1 cross-link (*N*-acetyl-*S*-[1-(3-((4-aminobutyl)amino)propyl)-1*H*-pyrrol-3-yl]-L-cysteine, NAC-BDA-N^1-spermidine, **12a**), whereas the compound that elutes at 37.1 min is the spermidine-N^8 cross-link (*N*-acetyl-*S*-[1-(4-((3-aminobutyl)amino)propyl)-1*H*-pyrrol-3-yl]-L-cysteine, NAC-BDA-N^8-spermidine, **12b**) (Scheme 3).

There were metabolites in the urine of furan-treated rats with retention times and molecular ions as well as fragmentation patterns identical to the synthetic standards (Figure 3, Table 1). These compounds were not present in the urine of vehicle-treated controls. The mass of the NAC-BDA-spermidine metabolites were increased by 4 mass units in the urine from [$^{13}C_4$]furan-treated rats (Figure 3, Table 1). Their identity was further verified by co-elution with the synthetic standards (Supplementary Figure 6) and by high resolution mass spectral analysis (Table 1).

Since we had observed sulfoxide derivatives of the NAC-BDA-lysine metabolites in urine from furan-treated rats,[11,12] we investigated the possibility that the NAC-BDA-spermidine cross-links also underwent oxidation to their corresponding sulfoxides. Standards for these metabolites were prepared by oxidizing each of the NAC-BDA-spermidine cross-links with *m*-chloroperbenzoic acid (mCPBA). The products of the oxidation had the expected molecular ion at *m/z* 373. NMR analysis of the products was performed to confirm that the oxidation had occurred on the sulfur atom. This analysis indicated that each peak was a mixture of two diastereomers in a 6:5 ratio major:minor (based on the orientation of the sulfoxide oxygen). The sulfoxides for NAC-BDA-N^1-spermidine eluted at 3.7 min (*N*-acetyl-*S*-[1-(3-(4-aminobutylamino)propyl)-1*H*-pyrrol-3-yl]-L-cysteine sulfoxide), whereas the sulfoxides for NAC-BDA-N^8-spermidine eluted at 3.5 min (*N*-acetyl-*S*-[1-(4-(3-aminobutylamino)propyl)-1*H*-pyrrol-3-yl]-L-cysteine sulfoxide). Given that these compounds eluted very early and there were co-eluting peaks with the same mass, it was difficult to judge whether these compounds were formed in vivo.

To look for evidence for the possible presence of NAC-BDA-putrescine or further metabolites of NAC-BDA-ornithine or NAC-BDA-spermidine, urine from furan- and

vehicle-treated rats were analyzed by CNL scanning using a triple quadrupole mass spectrometer. Both CNL 129 (for the NAC conjugates) and CNL 177 (for NAC sulfoxides) were performed.[11] These studies did not lead to the identification of additional metabolites beyond NAC-BDA-spermidine (data not shown).

Relative Formation of GSH-BDA-Amines

In rat hepatocytes, the relative abundance of GSH-BDA-amine reaction products was GSH-BDA-N^{δ}-ornithine > GSH-BDA-N^{α}-ornithine ≥ GSH-BDA-N^{ε}-lysine and its acetylated counterpart ≥ GSH-BDA-N^{1}-spermidine > GSH-BDA-N^{8}-spermidine > GSH-BDA-N^{α}-lysine > GSH-BDA-putrescine. Neither GSH-BDA-spermine nor GSH-BDA-cadaverine was observed. To determine the relative reactivity of GSH-BDA (**3**) with these various amines, 5 mM GSH was reacted with 100 μM BDA and an equimolar mixture of the amines (100 μM each putrescine, cadaverine, spermine, spermidine, ornithine, and lysine) in either 150 mM sodium phosphate buffer (pH 7.4) or in hepatocyte medium (RPMI 1640 media, containing 10 mM HEPES, pH 7.4). The reaction was allowed to proceed for 90 min at 37 °C before analysis by LC/MS using an ion trap mass spectrometer as a detector (Figure 4). The peak areas were corrected for ionization efficiency (Supplemental Table 1). The results of these experiments are summarized in Figure 5. The expected products are shown in Scheme 2. In addition to GSH-BDA cross-links to putrescine, cadaverine, spermine, spermidine, ornithine, and lysine, intramolecular and intermolecular cross-links to GSH were also formed (mono-GSH-BDA, **4**, and GSH-BDA-GSH, **13**; Scheme 2).

The relative amount of each reaction product formed was dependent on the nature of the buffer. In 150 mM sodium phosphate, pH 7.4, the most abundant product was GSH-BDA-GSH. The relative abundance of the amino acid and polyamine reaction products was GSH-BDA-spermine > GSH-BDA-N^{1}-spermidine ≥ GSH-BDA-putrescine ≥ GSH-BDA-N^{δ}-ornithine ≥ GSH-BDA-cadaverine > GSH-BDA-N^{8}-spermidine > GSH-BDA-N^{ε}-lysine > GSH-BDA-N^{α}-lysine ⋙ GSH-BDA-N^{α}-ornithine (not detected). In hepatocyte medium, the most abundant product was GSH-BDA-spermine. Only low levels of GSH-BDA-GSH were formed in this reaction buffer. The order of reaction was GSH-BDA-spermine > GSH-BDA-N^{1}-spermidine > GSH-BDA-putrescine > GSH-BDA-N^{8}-spermidine > GSH-BDA-cadaverine > GSH-BDA-N^{ε}-lysine > GSH-BDA-N^{δ}-ornithine > GSH-BDA-N^{α}-lysine ⋙ GSH-BDA-N^{α}-ornithine (not detected). Upon summing together the regioisomers formed from each amine, the relative order of reactivity was spermine > spermidine > putrescine ≥ ornithine ≈ lysine ≈ cadaverine in both reaction solvents.

The overall yield of the reaction products was lower when the reaction was performed in hepatocyte medium (Figure 4). The medium contains many chemicals that are likely to compete with the amines (including the amino group of GSH) for reaction with BDA or GSH-BDA (**3**), reducing the overall yield of cross-links. A major reaction product was observed in the hepatocyte media reaction that was not present in the buffer reaction mixture. This compound eluted at 33.9 min and had a molecular ion at *m/z* 477. This compound was formed in the absence of the amine mixture but required BDA, GSH and the media. The formation of this compound likely competes with production of the GSH-BDA-amine cross-links. The chemical structure of this compound was not determined. The daughter ion mass spectrum indicated that it was a reaction product containing GSH since it contained ions resulting from neutral losses characteristic of GSH (NL 75 and 129). This compound is not likely a GSH-BDA-amine cross-link since there are no amines present in the hepatocyte medium that would generate a GSH-BDA-amine cross-link with the correct mass. Additionally, the MS^2 spectrum of the unknown contained an ion which indicates the neutral loss of GSH (neutral loss of 307). This fragmentation is not observed in any of the GSH-BDA-amine cross-links characterized to date.

Further evidence that the presence of additional nucleophiles affects the product distribution was provided by comparing the regioselectivity of the reaction of GSH-BDA (**3**) with ornithine, lysine and spermidine (Table 2) between the different reaction settings. In the in vitro reaction with the amine mixture, the GSH-BDA-N^{α}-ornithine cross-link was not detected. However, both the α- and δ-ornithine reaction products were observed when ornithine was reacted with GSH and BDA alone, with the reaction still preferentially occurring with the δ-amino group. The nature of the reaction buffer did not influence the relative product formation for this amino acid. There was a slight effect of reaction medium on the relative reactivity of the N^{α}- and N^{ε}-amino groups of lysine. The preference of reaction with the N^{ε}-amino group has been previously reported.[11] There was also significant regioselectivity in the reaction of BDA-GSH with the two amino groups of spermidine with the reaction preferentially occurring on the N^{1} nitrogen atom. For this amine, the reaction medium significantly influences the relative reactivity of the two amino groups.

DISCUSSION

Previously we demonstrated that a significant route of furan metabolism involves the oxidation of furan to BDA, followed by reaction of BDA with GSH to form GSH-BDA (**3**) that can cross-link with amines like lysine and glutamine.[11,12] In this report, we characterized GSH-BDA-ornithine, GSH-BDA-spermidine and GSH-BDA-putrescine as hepatocyte metabolites of furan. These compounds indicate that any endogenous amine could be a target for alkylation by GSH-BDA (**3**). More importantly, they may signify that polyamines have an important function in the toxicity of furan.

To our knowledge, this is the first identification of xenobiotic-polyamine adducts in a cell- or animal-based system. The formation of these products demonstrates that polyamines serve as traps for electrophiles, detoxifying the reactive aldehydes formed during furan metabolism and preventing them from modifying proteins or other critical targets. This protection is expected to dominate at lower furan exposures, where the concentrations of GSH-BDA (**3**) are likely insufficient to result in significant depletion of polyamines. Polyamines are known to protect against oxidative damage, radiation damage and alkylation damage by a variety of mechanisms.[23-30] Mechanisms for protection include direct scavenging of the reactive molecule, induction of conformational changes in DNA, physical blocking of DNA from interactions with the reactive intermediate, or a combination of all four. Until this report, the products of these scavenging reactions have only been chemically characterized in vitro.[23,26,30]

These products could also represent adverse effects for furan-exposed cells since polyamines play a vital role in cellular homeostasis. They are essential for a wide variety of cellular functions including cell growth and differentiation.[31-33] Therefore at high furan exposure, one might envision that the formation of GSH-BDA-polyamine adducts might significantly alter the balance of polyamines in the liver. Changes in the polyamine pools have a major influence on cellular physiology; consequently their levels are tightly regulated through altered expression of the enzymes involved in their synthesis and degradation.[32] Increased polyamine levels are associated with increased cell proliferation, decreased apoptosis and increased expression of oncogenic genes.[14] An exception to this is that extremely high levels of polyamines leads to apoptosis.[14] Alternatively, decreased polyamine levels are associated with decreased cell growth and apoptosis.[16,29,34,35] Therefore, if furan disrupts these polyamine pools via the formation of GSH-BDA-polyamine metabolites, these changes could play an important role in the overall toxicological effects of furan.

It is also possible that the products of these reactions, GSH-BDA-polyamine, are themselves toxic. Polyamine analogs have been explored for their potential as antitumor agents.[36] A

number of these compounds are cytotoxic at submicromolar concentrations, so it is possible that the analogs we are detecting as a result of furan metabolism may have toxic properties. Taken together, it is possible that the modification of polyamines by reactive intermediates in furan metabolism could play an important role in furan-derived toxicity by disturbing the polyamine pools, triggering compensatory changes in enzyme levels to replace modified polyamines, and/or altering the biological activity of polyamines as a result of chemical modification of the terminal amino group. These possibilities are currently being explored.

A critical step in understanding the potential importance of these metabolites to the toxicity of furan is defining patterns of reactivity of GSH-BDA (**3**) in various biologically relevant contexts. The relative amount of product formed in hepatocytes is GSH-BDA-ornithine > GSH-BDA-lysine > GSH-BDA-spermidine ≫ GSH-BDA-putrescine. GSH-BDA-spermine and GSH-BDA-cadaverine were not observed. The only GSH reaction product was mono-GSH-BDA (**4**), not GSH-BDA-GSH (**13**). Our chemical studies indicate that there are multiple factors that influencing the cross-link product distribution in the isolated hepatocytes. They include the relative concentration of the amines in hepatocytes, the relative reactivity of the amino groups, and the presence of competing nucleophiles. Biochemical stability of the resulting products will also affect the amounts detected.

As shown in Table 3, the absence of GSH-BDA-cadaverine can be explained by the extremely low hepatocellular cadaverine concentrations.[37] Similarly, the relatively low levels of GSH-BDA-putrescine are likely explained by the low amounts of putrescine present in hepatocytes.[38] However, amine hepatocellular concentrations do not explain the relative levels of GSH-BDA-lysine, GSH-BDA-ornithine, GSH-BDA-spermidine, GSH-BDA-spermine and GSH-BDA-GSH. Given the reported hepatocellular levels of these amines (Table 3),[38-41] one would predict that the relative hepatocellular levels of these conjugates should be GSH-BDA-GSH > GSH-BDA-spermine ≈ GSH-BDA-spermidine > GSH-BDA-lysine ≥ GSH-BDA-ornithine. Since the relative distribution of these metabolites is very different than this, factors other than relative concentration of the amines must play a role in the relative product distribution observed in hepatocytes.

One contributor to the product distribution could be the relative reactivity of the various biological amines. Our chemical studies indicated that relative reactivity was spermine > spermidine > putrescine ≥ ornithine ≈ lysine ≈ cadaverine in both reaction solvents. These data show that primary amines attached to alkyl chains are preferred over primary amines that are α to a carboxylic acid as reaction partners of the dialdehyde GSH-BDA (**3**). This preference can be attributed to electronic and steric effects. It accounts for why the GSH-BDA-polyamine cross-links are major reaction products despite a 50-fold excess of GSH over any individual amine (the primary amino group of GSH is α to a carboxylic acid, and is therefore relatively unreactive). It also explains why the terminal amino groups of lysine and ornithine are preferred over the corresponding α-amino group. These observations are consistent with previous studies which demonstrated that α,β-unsaturated aldehydes react with spermine > spermidine > putrescine ≥ N^{ε}-lysine > N^{α}-amine of amino acids.[30,42]

Another factor influencing product distribution could be the pK_a of the individual amino groups since the protonation state of a primary amine is an important factor determining its nucleophilicity.[43] While the relative reactivity of the amines with GSH-BDA (**3**) does not strictly correlate to their pK_a's (Table 3), relative pK_a's can be used to justify reactivity when looking at structurally related pairs. For example, putrescine has a pK_a of 9.63 versus cadaverine with a pKa of 10.05 (Table 3). Therefore, a greater fraction of putrescine will be unprotonated and available for nucleophilic attack, justifying its greater extent of product formation in comparison with cadaverine in our model reactions. In contrast, the lower pK_a's of the α-amino groups do not lead to greater reaction at this position compared to the

side-chain amines for reasons discussed above. Therefore the utility of analysis based on pK_a is limited to the consideration of structurally related molecules. Stability of reaction intermediates may also influence product distribution.

The regiochemistry of the reaction of GSH-BDA (**3**) with ornithine, spermidine and lysine in hepatocytes reflected the relative reactivity of these amino groups in the chemical reactions (Table 2). In hepatocytes, the reaction of GSH-BDA (**3**) was more skewed to the ε-amino group of lysine than in the in vitro reactions. As previously reported, there are two possible sources of GSH-BDA-lysine: one is the reaction of GSH-BDA (**3**) with free lysine and the other is the degradation and processing of GSH-BDA-lysine protein adducts.[11] The latter adduct will only lead to GSH-BDA-N^{ε}-lysine since the α-amino group is involved in peptide bonds, explaining the observed α/ε ratio observed in hepatocytes.[11]

Regiochemistry aside, differences in chemical reactivity of the amines with GSH-BDA (**3**) do not explain the relative levels of GSH-BDA-lysine, GSH-BDA-ornithine, GSH-BDA-spermidine, GSH-BDA-spermine and GSH-BDA-GSH observed in hepatocytes. Another factor that could contribute to the hepatocyte product distribution is the chemical make up of the reaction site, as indicated by the difference in total product yields obtained in sodium phosphate buffer versus hepatocyte medium. The presence of competing nucleophiles reduced the formation of GSH-BDA-GSH in hepatocyte medium (Figure 5). This reduction was accompanied by the abundant formation of a medium component-derived reaction product (*m/z* 477). Therefore, it is likely that GSH-BDA-GSH is not observed in furan-exposed hepatocytes because there are many nucleophiles that could compete with GSH's glutamyl amino group for reaction with GSH-BDA (**3**) in the cell. A similar argument can be made for the difference in regioselectivity in the formation of GSH-BDA-spermidine regioisomers, although this difference could also be explained by differences in pH or ion strength of the reaction media.[43] However, the presence of additional nucleophiles will compete with amines for reaction with GSH-BDA (**3**) so that the reactive metabolite will combine with the most reactive ones first. This hypothesis also may explain the enhanced regioselectivity of the reaction of GSH-BDA (**3**) with spermidine in the hepatocyte medium versus sodium phosphate and with ornithine when multiple amines are present (Table 2). However, it does not provide insight into the absence of GSH-BDA-spermine and the relative amounts of GSH-BDA-spermidine, GSH-BDA-ornithine and GSH-BDA-lysine detected in rat hepatocytes.

Since the chemical reactions indicate that spermine and spermidine are very reactive with GSH-BDA (**3**), it is surprising that GSH-BDA-spermine was not detected and that the levels of GSH-BDA-spermidine are lower than those observed for GSH-BDA-lysine and GSH-BDA-ornithine. It is possible that spermine and spermidine may not be readily available for reaction with GSH-BDA (**3**) since their free concentration is substantially lower than the total cellular polyamine concentration.[32] The possibility that these products are formed but sequestered within the hepatocyte was eliminated by the absence of these products in deproteinized cell lysates (data not shown). A likely possibility is that GSH-BDA-spermine is formed but rapidly degraded to GSH-BDA-spermidine by enzymes in the cell, such as amine oxidases.[32,44] A similar mechanism could explain the lower than expected amounts of GSH-BDA-spermidine. These degradation reactions produce hydrogen peroxide and aldehydes known to be toxic to cells.[16] The metabolism of these conjugates could be responsible for the oxidative stress observed in liver following furan treatment.[45] We observed that GSH-BDA-spermidine was unstable in the hepatocyte incubations with the N^1-isomer more unstable than the N^8-isomer (data not shown). This instability was not observed in the absence of cells. The biological fate of these metabolites requires investigation.

The only downstream metabolite of these newly characterized GSH-BDA-amine products that was detected in urine of furan-treated rats was NAC-BDA-spermidine. The lack of detection of NAC-BDA-putrescine in the urine of furan-treated rats is not surprising since only low levels of this metabolite were detected in hepatocytes. Given the large abundance of GSH-BDA-ornithine in furan-treated rat hepatocytes, it is surprising that there were no detectable levels of NAC-BDA-ornithine in rat urine following furan exposure. Further studies will be necessary to determine if GSH-BDA-ornithine is formed in vivo and, if so, what its fate is.

The urinary levels of NAC-BDA-spermidine appeared to be much lower than those of NAC-BDA-lysine and related metabolites based on MS analysis. While this observation could result from large differences in ionization efficiency of the two metabolites in the mass spectrometer, a more likely possibility is that CYS-BDA-lysine cross-links dominate in vivo since a major source of this cross-link is likely to be BDA-derived protein adducts.[11] Thirteen percent of an 8 mg/kg dose of furan becomes bound to proteins[46], therefore the degradation products of these adducts are expected to dominate in the urine and feces of furan-treated rodents.[10,11,47] Future studies will focus on the development of analytical methods to quantify each of the metabolites detected in the urine of furan-treated rats to get a better sense of the overall mass balance of the various pathways.

In summary, GSH-BDA-amine cross-links with ornithine, putrescine and spermidine were detected following exposure of rat hepatocytes to furan. Degradation products of the GSH-BDA-spermidine products were detected in low levels in urine of furan-treated rats. The high reactivity of GSH-BDA (**3**) with spermine and spermidine suggest that the formation of these conjugates could represent detoxification pathways at low furan exposures. At higher exposure levels, these reactions may cause imbalances in polyamine metabolism through a variety of mechanisms. Imbalances in polyamine metabolism have been linked to cancer and cell death.[16] These furan metabolites may be important clues into the mechanisms by which furan causes its harmful effects.

Supplementary Material

Refer to Web version on PubMed Central for supplementary material.

Acknowledgments

We thank Anna Urban, Patrick Kinney, Dr. Fekadu Kassie, and Dr. Michael Byrns for their assistance with the animal studies, Dr. Peter Villalta and Brock Matter for their assistance with the mass spectral analyses and Choua Vu for the synthesis of [$^{13}C_4$]furan.

Funding Sources The Analytical Biochemical Core at the Masonic Cancer Center, University of Minnesota is funded by National Cancer Institute Center Grant CA-77598. NMR instrumentation was provided with funds from the NSF (BIR-961477), the University of Minnesota Medical School, and the Minnesota Medical Foundation. This research was funded by ES-10577 from the National Institutes of Health. Martin Phillips is funded by a fellowship from the Department of Medicinal Chemistry, University of Minnesota.

Reference List

1. National Toxicology Program. Toxicology and carcinogenesis studies of furan in F344/N rats and B6C3F$_1$ mice vol NTP Technical Report No 402. US Department of Health and Human Services, Public Health Service, National Institutes of Health; Research Triangle Park, NC: 1993.
2. International Agency for Research on Cancer. Dry Cleaning, Some Chlorinated Solvents and Other Industrial Chemicals. IARC; Lyon, France: 1995. Furan; p. 393
3. Perez LC, Yaylayan VA. Origin and mechanistic pathways of formation of the parent furan--a food toxicant. J Agric Food Chem. 2004; 52:6830–6836. [PubMed: 15506823]

4. National Toxicology Program. 11th Report on Carcinogens. US Department of Health and Human Services; Washington DC: 2005.
5. Carfagna MA, Held SD, Kedderis GL. Furan-induced cytolethality in isolated rat hepatocytes: Correspondence with *in vivo* dosimetry. Toxicol Appl Pharmacol. 1993; 123:265–273. [PubMed: 8248933]
6. Mugford CA, Carfagna MA, Kedderis GL. Furan-mediated uncoupling of hepatic oxidative phosphorylation in Fischer-344 rats: an early event in cell death. Toxicol Appl Pharmacol. 1997; 144:1–11. [PubMed: 9169064]
7. Chen LJ, Hecht SS, Peterson LA. Identification of *cis*-2-butene-1,4-dial as a microsomal metabolite of furan. Chem Res Toxicol. 1995; 8:903–906. [PubMed: 8555403]
8. Peterson LA, Cummings ME, Vu CC, Matter BA. Glutathione trapping to measure microsomal oxidation of furan to *cis*-2-butene-1,4-dial. Drug Metab Dispos. 2005; 33:1453–1458. [PubMed: 16006568]
9. Peterson LA, Cummings ME, Chan JY, Vu CC, Matter BA. Identification of a *cis*-2-butene-1,4-dial-derived glutathione conjugate in the urine of furan-treated rats. Chem Res Toxicol. 2006; 19:1138–1141. [PubMed: 16978017]
10. Kellert M, Wagner S, Lutz U, Lutz WK. Biomarkers of furan exposure by metabolic profiling of rat urine with liquid chromatography-tandem mass spectrometry and principal component analysis. Chem Res Toxicol. 2008; 21:761–768. [PubMed: 18269250]
11. Lu D, Sullivan MM, Phillips MB, Peterson LA. Degraded protein adducts of *cis*-2-butene-1,4-dial are urinary and hepatocyte metabolites of furan. Chem Res Toxicol. 2009; 22:997–1007. [PubMed: 19441776]
12. Lu D, Peterson LA. Identification of furan metabolites derived from cysteine-*cis*-2-butene-1,4-dial-lysine cross-links. Chem Res Toxicol. 2010; 23:142–151. [PubMed: 20043645]
13. Igarashi K, Kashiwagi K. Modulation of cellular function by polyamines. Int J Biochem Cell Biol. 2010; 42:39–51. [PubMed: 19643201]
14. Gerner EW, Meyskens FL Jr. Polyamines and cancer: old molecules, new understanding. Nat Rev Cancer. 2004; 4:781–792. [PubMed: 15510159]
15. Casero RA Jr, Marton LJ. Targeting polyamine metabolism and function in cancer and other hyperproliferative diseases. Nat Rev Drug Discov. 2007; 6:373–390. [PubMed: 17464296]
16. Casero RA, Pegg AE. Polyamine catabolism and disease. Biochem J. 2009; 421:323–338. [PubMed: 19589128]
17. Vu CC, Peterson LA. Synthesis of [$^{13}C_4$]furan. J Label Compounds Radiopharm. 2005; 48:117–121.
18. Byrns MC, Vu CC, Peterson LA. The formation of substituted 1,N^6-etheno-2'-deoxyadenosine and 1,N^2-etheno-2'-deoxyguanosine adducts by *cis*-2-butene-1,4-dial, a reactive metabolite of furan. Chem Res Toxicol. 2004; 17:1607–1613. [PubMed: 15606136]
19. Chen LJ, Hecht SS, Peterson LA. Characterization of amino acid and glutathione adducts of *cis*-2-butene-1,4-dial, a reactive metabolite of furan. Chem Res Toxicol. 1997; 10:866–874. [PubMed: 9282835]
20. Peterson LA, Naruko KC, Predecki D. A reactive metabolite of furan, *cis*-2-butene-1,4-dial, is mutagenic in the Ames assay. Chem Res Toxicol. 2000; 13:531–534. [PubMed: 10898583]
21. Berry MN, Friend DS. High-yield preparation of isolated rat liver parenchymal cells: a biochemical and fine structural study. J Cell Biol. 1969; 43:506–520. [PubMed: 4900611]
22. Wilkinson CF, Hetnarski K, Denison MS, Guengerich FP. Selectivity of 1-phenylimidazole as a ligand for cytochrome P-450 and as an inhibitor of microsomal oxidation. Biochem Pharmacol. 1983; 32:997–1003. [PubMed: 6838663]
23. Sava IG, Battaglia V, Rossi CA, Salvi M, Toninello A. Free radical scavenging action of the natural polyamine spermine in rat liver mitochondria. Free Radic Biol Med. 2006; 41:1272–1281. [PubMed: 17015174]
24. Tadolini B. Polyamine inhibition of lipoperoxidation. The influence of polyamines on iron oxidation in the presence of compounds mimicking phospholipid polar heads. Biochem J. 1988; 249:33–36. [PubMed: 3124824]

25. Lovaas E, Carlin G. Spermine: an anti-oxidant and anti-inflammatory agent. Free Radic Biol Med. 1991; 11:455–461. [PubMed: 1663062]
26. Ha HC, Sirisoma NS, Kuppusamy P, Zweier JL, Woster PM, Casero RA Jr. The natural polyamine spermine functions directly as a free radical scavenger. Proc Natl Acad Sci U S A. 1998; 95:11140–11145. [PubMed: 9736703]
27. Rider JE, Hacker A, Mackintosh CA, Pegg AE, Woster PM, Casero RA Jr. Spermine and spermidine mediate protection against oxidative damage caused by hydrogen peroxide. Amino Acids. 2007; 33:231–240. [PubMed: 17396215]
28. Belle NA, Dalmolin GD, Fonini G, Rubin MA, Rocha JB. Polyamines reduces lipid peroxidation induced by different pro-oxidant agents. Brain Res. 2004; 1008:245–251. [PubMed: 15145762]
29. Norikura T, Kojima-Yuasa A, Opare KD, Matsui-Yuasa I. Protective effect of gamma-aminobutyric acid (GABA) against cytotoxicity of ethanol in isolated rat hepatocytes involves modulations in cellular polyamine levels. Amino Acids. 2007; 32:419–423. [PubMed: 16937319]
30. Yoshida M, Tomitori H, Machi Y, Hagihara M, Higashi K, Goda H, Ohya T, Niitsu M, Kashiwagi K, Igarashi K. Acrolein toxicity: Comparison with reactive oxygen species. Biochem Biophys Res Commun. 2009; 378:313–318. [PubMed: 19032949]
31. Pignatti C, Tantini B, Stefanelli C, Flamigni F. Signal transduction pathways linking polyamines to apoptosis. Amino Acids. 2004; 27:359–365. [PubMed: 15452702]
32. Pegg AE. Mammalian polyamine metabolism and function. IUBMB Life. 2009; 61:880–894. [PubMed: 19603518]
33. Toninello A, Salvi M, Mondovi B. Interaction of biologically active amines with mitochondria and their role in the mitochondrial-mediated pathway of apoptosis. Curr Med Chem. 2004; 11:2349–2374. [PubMed: 15379717]
34. Wu C, Kennedy DO, Yano Y, Otani S, Matsui-Yuasa I. Thiols and polyamines in the cytoprotective effect of taurine on carbon tetrachloride-induced hepatotoxicity. J Biochem Mol Toxicol. 1999; 13:71–76. [PubMed: 9890191]
35. Schipper RG, Penning LC, Verhofstad AA. Involvement of polyamines in apoptosis. Facts and controversies: effectors or protectors? Semin Cancer Biol. 2000; 10:55–68. [PubMed: 10888272]
36. Casero RA Jr, Woster PM. Recent advances in the development of polyamine analogues as antitumor agents. J Med Chem. 2009; 52:4551–4573. [PubMed: 19534534]
37. Clements RL, Holt A, Gordon ES, Todd KG, Baker GB. Determination of rat hepatic polyamines by electron-capture gas chromatography. J Pharmacol Toxicol Methods. 2004; 50:35–39. [PubMed: 15233965]
38. Marce M, Brown DS, Capell T, Figueras X, Tiburcio AF. Rapid high-performance liquid chromatographic method for the quantitation of polyamines as their dansyl derivatives: application to plant and animal tissues. J Chromatogr B Biomed Appl. 1995; 666:329–335. [PubMed: 7633610]
39. Statter M, Russel A. Competitive interrelationships between lysine and arginine in rat liver under normal conditions and in experimental hyperammonemia. Life Sci. 1978; 22:2097–2101. [PubMed: 672448]
40. Yamashita K, Ashida K. Lysine metabolism in rats fed lysine-free diet. J Nutr. 1969; 99:267–273. [PubMed: 5350980]
41. Wahllander A, Soboll S, Sies H, Linke I, Muller M. Hepatic mitochondrial and cytosolic glutathione content and the subcellular distribution of GSH-*S*-transferases. FEBS Lett. 1979; 97:138–140. [PubMed: 761610]
42. Zhou S, Decker EA. Ability of carnosine and other skeletal muscle components to quench unsaturated aldehydic lipid oxidation products. J Agric Food Chem. 1999; 47:51–55. [PubMed: 10563848]
43. Smith, MB.; March, J. March's Advanced Organic Chemistry: Reactions, Mechanisms, and Structure. John Wiley & Sons; Hoboken, New Jersey: 2007. Effects of structure and medium on reactivity; p. 395-416.
44. Wang Y, Casero RA Jr. Mammalian polyamine catabolism: a therapeutic target, a pathological problem, or both? J Biochem. 2006; 139:17–25. [PubMed: 16428315]

45. Hickling KC, Hitchcock JM, Oreffo V, Mally A, Hammond TG, Evans JG, Chipman JK. Evidence of oxidative stress and associated DNA damage, increased proliferative drive, and altered gene expression in rat liver produced by the cholangiocarcinogenic agent furan. Toxicol Pathol. 2010; 38:230–243. [PubMed: 20124500]
46. Burka LT, Washburn KD, Irwin RD. Disposition of [^{14}C]furan in the male F344 rat. Journal of Toxicology & Environmental Health. 1991; 34:245–257. [PubMed: 1920528]
47. Hamberger C, Kellert M, Schauer UM, Dekant W, Mally A. Hepatobiliary toxicity of furan: identification of furan metabolites in bile of male f344/n rats. Drug Metab Dispos. 2010; 38:1698–1706. [PubMed: 20639435]
48. Dawson, RMC.; Elliott, DC.; Elliott, WH.; Jones, KM. Data for biochemical research. Clarendon Press; Oxford: 1986.
49. Prior RL, Clifford AJ, Visek WJ. Tissue amino acid concentrations in rats during acute ammonia intoxication. Am J Physiol. 1970; 219:1680–1683. [PubMed: 5485685]
50. Prior RL, Visek WJ. Effects of urea hydrolysis on tissue metabolite concentrations in rats. Am J Physiol. 1972; 223:1143–1149. [PubMed: 4654346]
51. Cochon AC, Gonzalez N, San Martin de Viale LC. Effects of the porphyrinogenic compounds hexachlorobenzene and 3,5-diethoxycarbonyl-1,4-dihydrocollidine on polyamine metabolism. Toxicology. 2002; 176:209–219. [PubMed: 12093617]
52. Watanabe S, Sato S, Nagase S, Shimosato K, Ohkuma S. Effects of methotrexate and cyclophosphamide on polyamine levels in various tissues of rats. J Drug Target. 1999; 7:197–205. [PubMed: 10680975]
53. Andersson AC, Henningsson S, Rosengren E. Formation of cadaverine in the pregnant rat. Acta Physiol Scand. 1979; 105:508–512. [PubMed: 110032]
54. Aikens D, Bunce S, Onasch F, Parker R, Hurwitz C, Clemans S. The interactions between nucleic acids and polyamines .2. Protonation constants and C-13 NMR chemical-shift assignments of spermidine, spermine, and homologs. Biophysical Chemistry. 1983; 17:67–74. [PubMed: 6186302]
55. Sies H, Gerstenecker C, Menzel H, Flohe L. Oxidation in the NADP system and release of GSSG from hemoglobin-free perfused rat liver during peroxidatic oxidation of glutathione by hydroperoxides. FEBS Lett. 1972; 27:171–175. [PubMed: 11946832]
56. Sies, H.; Brigelius, R.; Akerboom, TPM. Intrahepatic Glutathione Status. In: Larsson, A.; Orrenius, S.; Holmgren, A.; Mannervik, B., editors. Functions of Glutathione: Biochemical, Physiological, Toxicological and Clinical Aspects. Raven Press; New York: 1983. p. 51-64.

Abbreviations

HRMS	High resolution mass spectrometry
BDA	*cis*-2-butene-1,4-dial
GSH-BDA	2-(*S*-glutathionyl)succinaldehyde
NAC	*N*-acetyl-L-cysteine
SRM	selective reaction monitoring
CNL	constant neutral loss
mCPBA	*m*-chloroperbenzoic acid

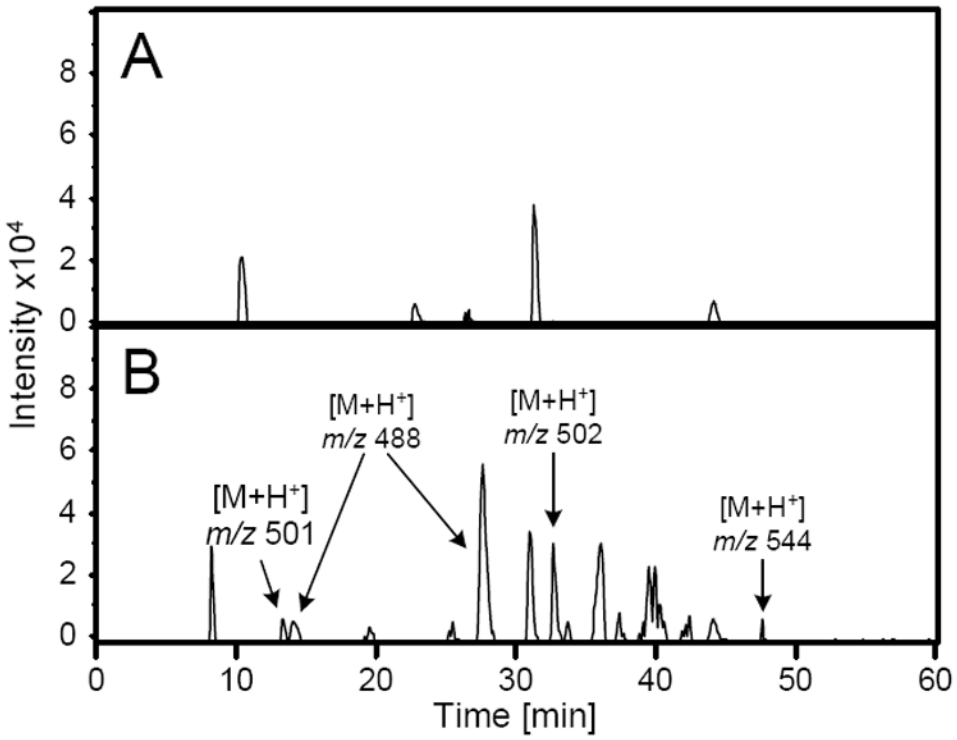

Figure 1.

Mass chromatogram generated upon extraction of the CNL 129 ion current from LC/MS/MS analysis of media from A) 0 or B) 100 μM furan-treated rat hepatocytes (HPLC method 1 with 10 mM ammonium formate, pH 2.8) obtained on an Agilent ion trap mass spectrometer. Previously characterized metabolites are *m/z* 502 (GSH-BDA-lysine) and *m/z* 544 (GSH-BDA-N^{α}-acetyl-lysine).[11] Unknowns are: *m/z* 488 and *m/z* 501.

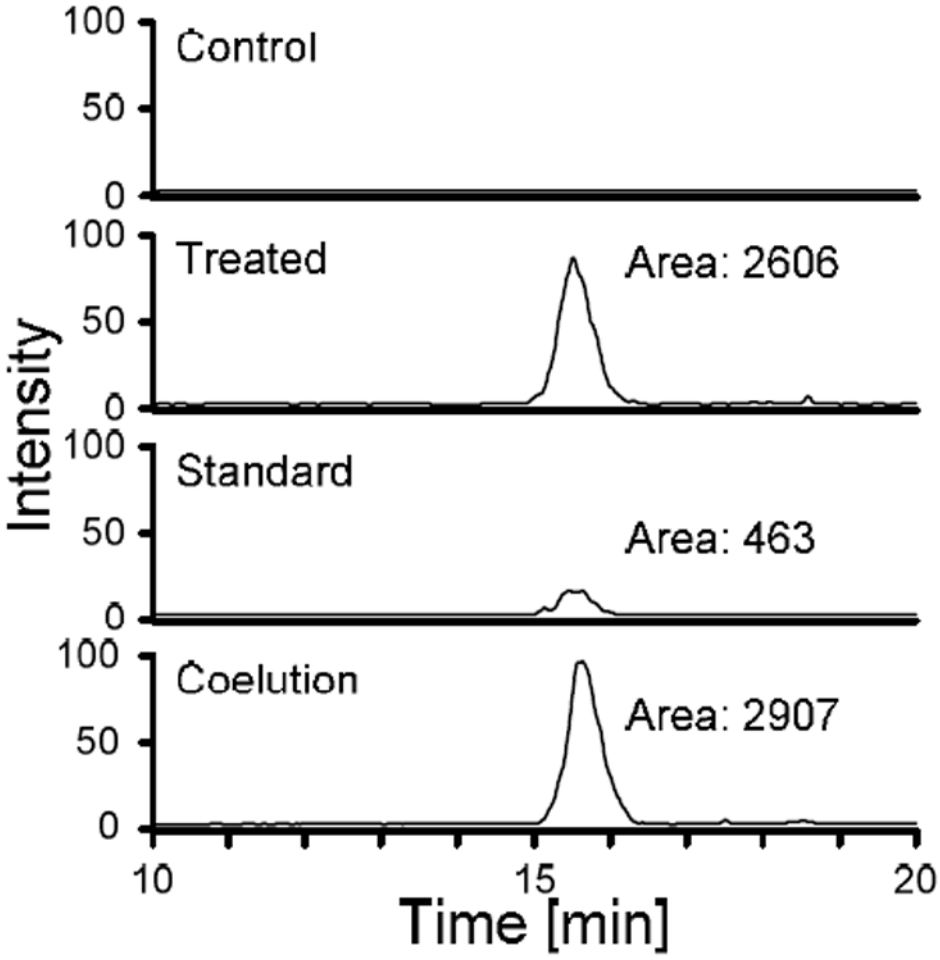

Figure 2.
LC/ESI-MS/MS analysis of media from furan- and control-treated hepatocytes for GSH-BDA-putrescine in the absence and presence of synthetic standard. The traces were generated by monitoring for the neutral loss of 129 from the molecular ion (*m/z* → 444 *m/z* 315).

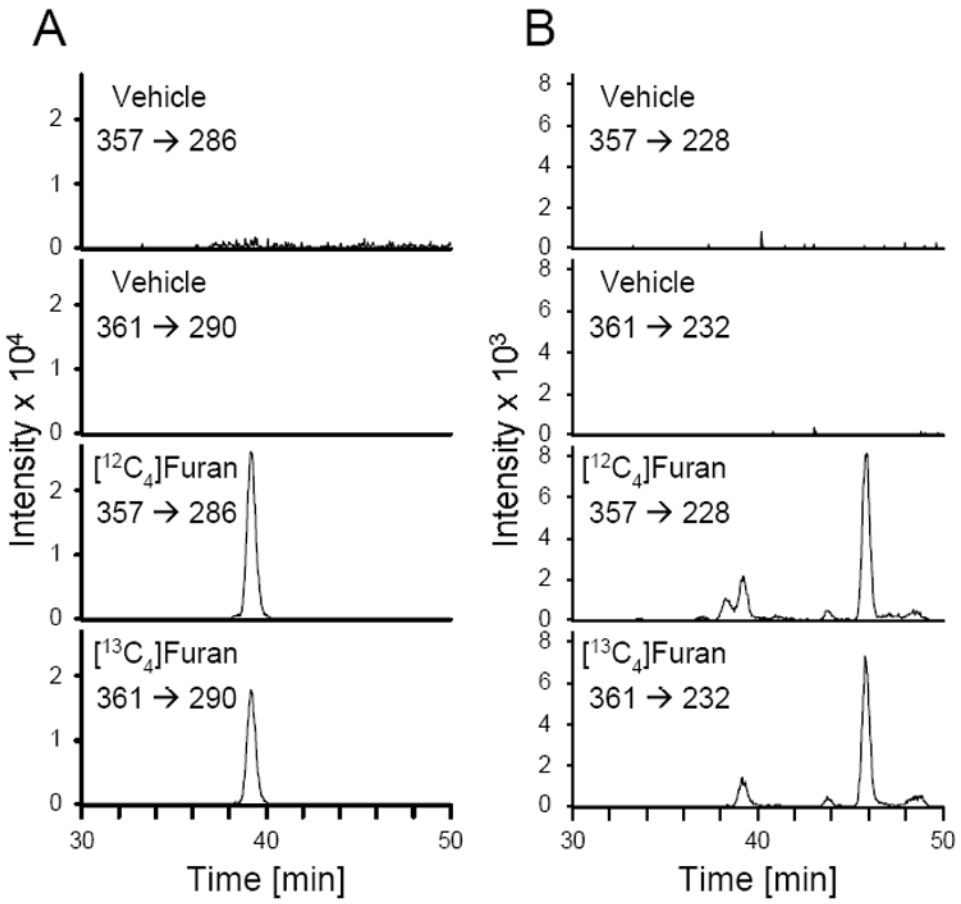

Figure 3.

LC/ESI-MS/MS analysis of rat urine for NAC-BDA-spermidine cross-links. Animals were treated with either corn oil alone or corn oil containing [$^{12}C_4$]- or [$^{13}C_4$]furan. A. The traces were generated by monitoring for the neutral loss of 71 from the molecular ion ([$^{12}C_4$]: *m/z* 357 → *m/z* 286; [$^{13}C_4$]: *m/z* 361 → *m/z* 290). B. The traces were generated by monitoring for the neutral loss of 129 from the molecular ion ([$^{12}C_4$]: *m/z* 357 → *m/z* 228; [$^{13}C_4$]: *m/z* 361 → *m/z* 232).

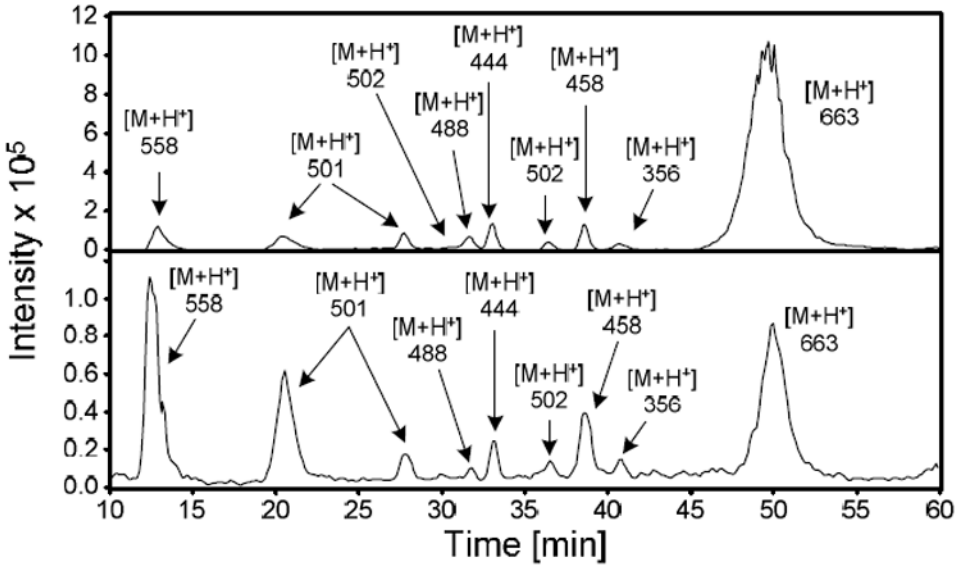

Figure 4.

Representative mass chromatograms of solutions of 5 mM GSH, 100 μM BDA and an equimolar mixture of the amines (100 μM each putrescine, cadaverine, spermine, spermidine, ornithine, and lysine) in either 150 mM sodium phosphate, pH 7.4, (top) in hepatocyte media (RPMI 1640 media containing 10 mM HEPES, pH 7.4, bottom).

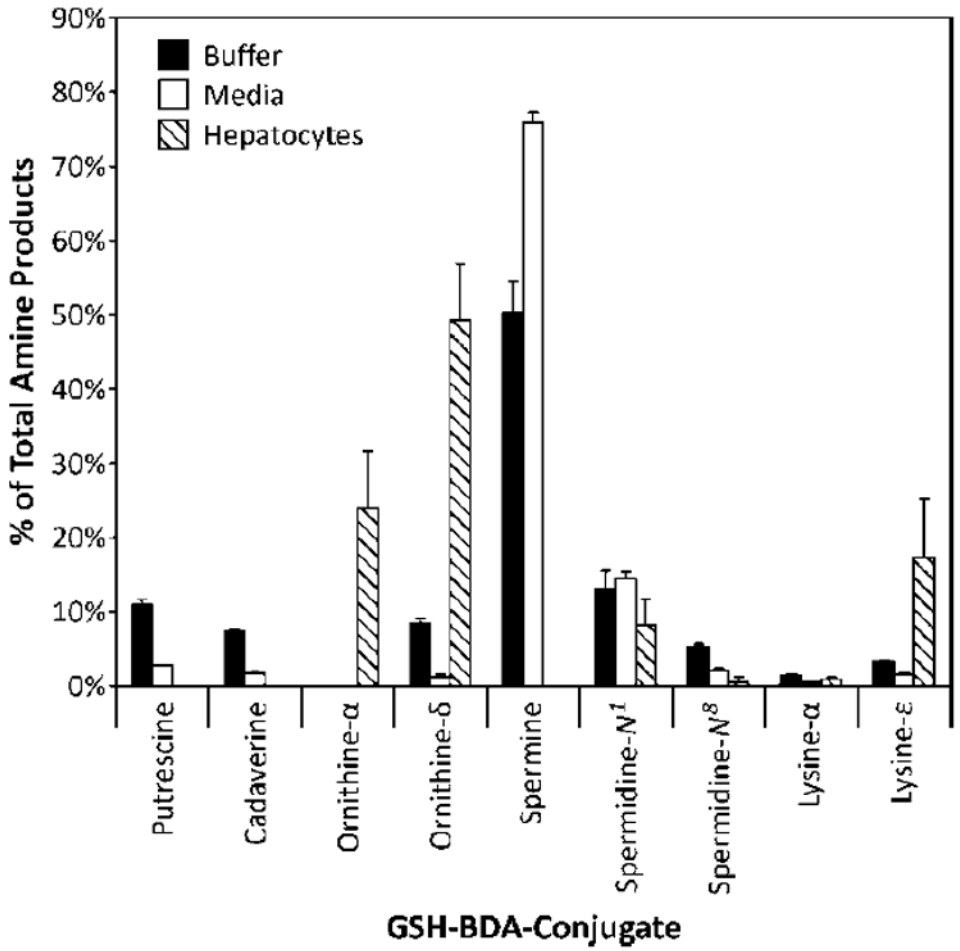

Figure 5.

Relative distribution of GSH-BDA-amine products in sodium phosphate, pH 7.4, hepatocyte media, and media from furan-treated rat hepatocytes as determined by LC-MS analysis. The amount of GSH-BDA-N$^{\alpha}$-lysine (**2b**) in furan treated-hepatocytes was calculated from the relative amount of **2b/2a** analysis using SRM monitoring.[11]

*Includes N^{α}-acetyl-L-lysine derivative of GSH-BDA-lysine.

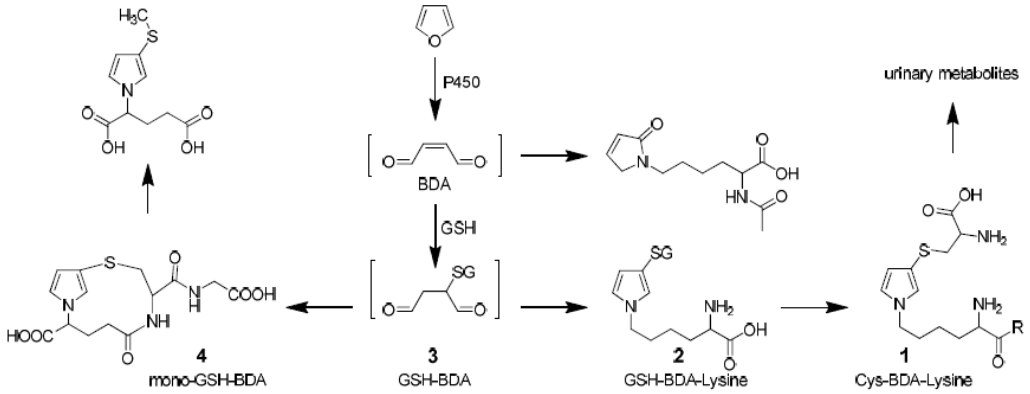

Scheme 1.
Major pathways of furan biotransformation in rats.

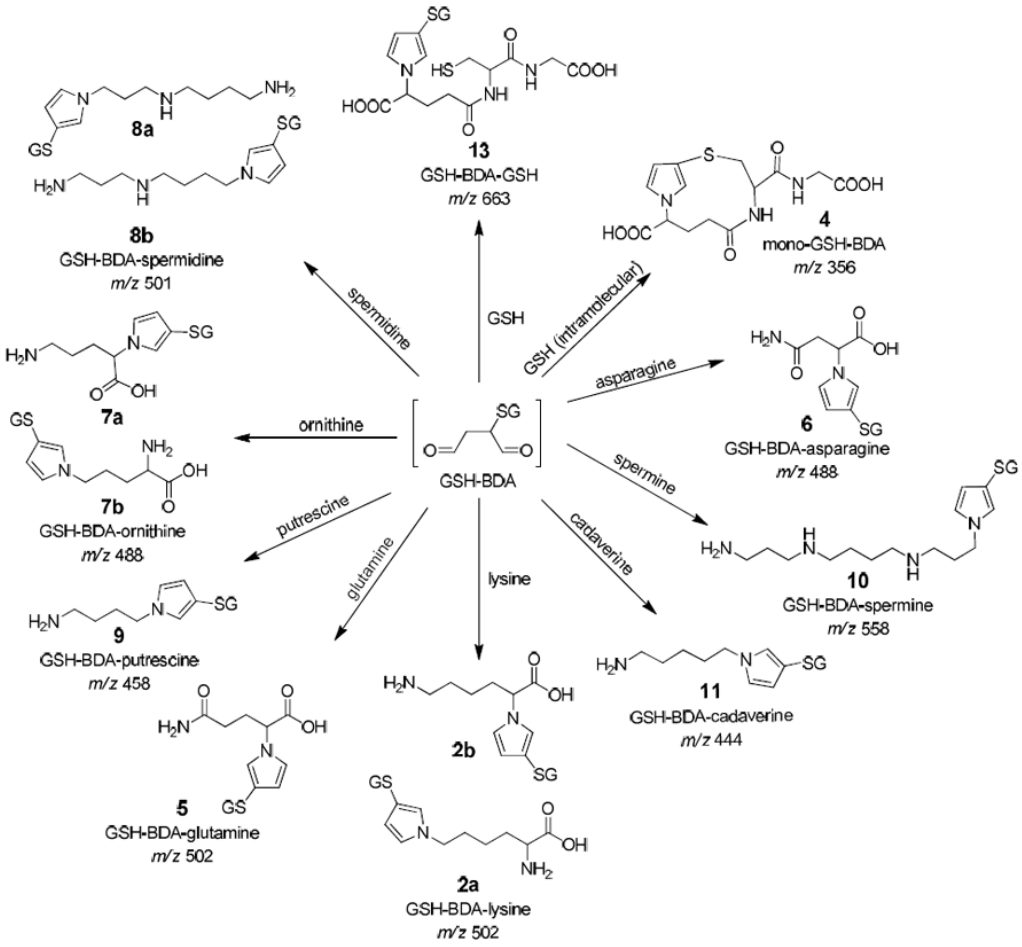

Scheme 2.
The reaction products formed when GSH-BDA is reacted with a variety of cellular amines.

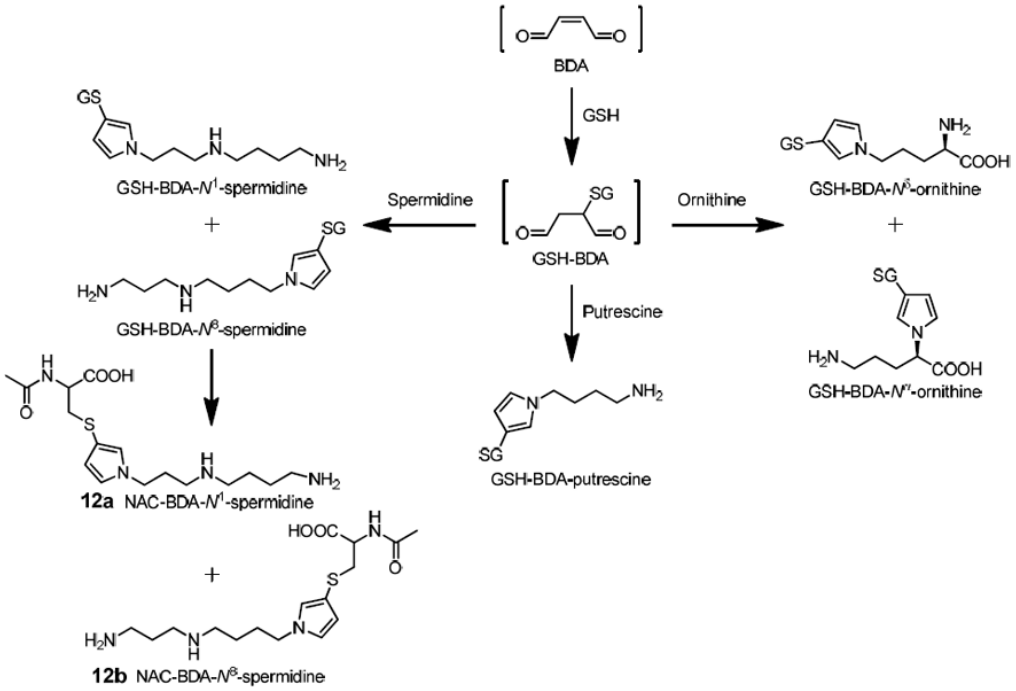

Scheme 3.

Proposed pathways of furan metabolism. GSH: L-Glutathione; NAC: *N*-Acetyl-L-cysteine

Table 1

Mass spectral data for the metabolites and standards.

Compound	*m/z*	RT[b](min)	MS^2 (fragment ions, *m/z*)	HRMS measured[a]	HRMS calculated
GSH-BDA-N^{α}-ornithine standard **7a**	488	24.4	470, 452, 359, 341	488.1806	488.1810
Hepatocyte metabolite	488	24.4	470, 452, 359, 341	488.1813	488.1810
GSH-BDA-N^{δ}-ornithine standard **7b**	488	31.8	470, 359, 342, 227, 213	488.1815	488.1810
Hepatocyte metabolite	488	31.9	470, 359, 342, 227, 213	488.1825	488.1810
GSH-BDA- N^1-spermidine standard **8a**	501	23.7	483, 372, 355, 301,227	501.2489	501.2490
Hepatocyte metabolite	501	23	483, 372, 355, 301, 227	n.d.[c]	501.2490
GSH-BDA-N^8-spermidine standard **8b**	501	28.4	483, 372, 228	501.2491	501.2490
Hepatocyte metabolite	501	28.5	483, 372, 228	n.d.	501.2490
GSH-BDA-putrescine **9**	444	34.4	426, 315	444.1890	444.1911
Hepatocyte metabolite	444	34.4	n.d.	n.d.	444.1911
GSH-BDA-cadaverine standard **11**	458	41.6	440, 329	458.2051	458.2068
GSH-BDA-spermine standard **10**	558	19.6	540, 429, 355, 285	558.3085	558.3068
NAC-BDA-N^{α}-ornithine standard	344	37.2	326, 308, 266, 221, 197	n.d.	344.1275
NAC-BDA-N^{δ}-ornithine standard	344	50.5	326, 308, 280, 215	n.d.	344.1275
NAC-BDA-N^1-spermidine standard **12a**	357	32.2	340, 322, 286, 268, 250, 211, 140	357.1939	357.1955
[$^{12}C_4$]Urinary metabolite	357	35.4	340, 322, 286, 268, 250, 211, 140	357.1948	357.1955
[$^{13}C_4$]Urinary metabolite	361	35.4	344, 326, 290, 272, 254, 215, 144		
NAC-BDA-N^8-spermidine standard **12b**	357	37.1	340, 300, 228	357.1958	357.1955
[$^{12}C_4$]Urinary metabolite	357	38.9	340, 300, 228	n.d.	357.1955
[$^{13}C_4$]Urinary metabolite	361	38.9	344, 304, 232		
NAC-BDA-N^1-spermidine sulfoxide standard	373	7.8	373, 244, 226, 155, 122	373.1913	373.1904
NAC-BDA-N^8-spermidine sulfoxide standard	373	8.2	373, 244, 226, 193, 176	373.1922	373.1904

[a] $[M+H^+]$ (*m/z*),

[b] RT = retention time;

[c] n.d. = not determined.

Data was acquired using HPLC Method 1 with 10 mM ammonium formate, pH 2.8.

Table 2

Regioselectivity of the reaction between GSH-BDA and ornithine, lysine or spermidine

	Amine mixture[a]		Individual amines[b]		
Amine	**Buffer**	**Media**	**Buffer**	**Media**	**Hepatocytes**
N^{α}/N^{δ} ornithine (**7a/7b**)	0	0	0.47	0.55	0.51 ± 0.17
N^{1}/N^{8} spermidine (**8a/8b**)	2.5 ± 0.3	6.9 ± 0.6	2.6	7.8	5.5 ± 1.8
$N^{\alpha}/N^{\varepsilon}$ lysine (**2b/2a**)	0.45 ± 0.05	0.26 ± 0.06	0.57	0.37	0.083 ± 0.021[c]

[a] GSH (5 mM) was combined with 100 μM BDA and an equimolar mixture of amines (100 μM each putrescine, cadaverine, spermine, spermidine, ornithine, and lysine) in either 150 mM sodium phosphate, pH 7.4 (buffer) or RPMI 1640 media, containing 10 mM HEPES, pH 7.4 (media). The reaction mixture was analyzed by LC-MS and the resultant peak areas were corrected for the ionization efficiency of each reaction product (Supplemental Table 1) prior to calculating the ratio of the two possible regioisomers.

[b] GSH (5 mM) was combined with 100 μM BDA and 100 μM ornithine, lysine or spermidine in either 150 mM sodium phosphate, pH 7.4 (buffer) or RPMI 1640 media, containing 10 mM HEPES, pH 7.4 (media). The reaction mixtures were analyzed as described above.

[c] Previously published.[11]

Table 3

Cellular amines pK_as and their concentrations in hepatocytes.

Amine	pK_a of amine	Conc. (nmol/g)
Ornithine	N^{α}: 8.69; N^{δ}:10.76[48]	230-370[39,49,50]
Lysine	N^{α}: 9.06; N^{ε}:10.54[48]	200-730[40,49,50]
Putrescine	9.63; 10.80[48]	18-57[37,38,51,52]
Cadaverine	10.05; 10.93[48]	2.6-7.9[37,53]
Spermine	10.1; 10.9[54]	618-1591[38,51,52]
Spermidine	N^{1}: 10.9; N^{8}: 9.9[54]	646-2205[37,38,51,52]
GSH	8.75[48]	5000-7000[55,56]